© 2016. Published by The Company of Biologists Ltd | Journal of Cell Science (2016) 129, 3238-3250 doi:10.1242/jcs.188870

RESEARCH ARTICLE

Microtubule-independent secretion requires functional maturation of Golgi elements

Lou Fourriere[1,2,3], Severine Divoux[1,2], Mila Roceri[1,2], Franck Perez[1,2,*,‡] and Gaelle Boncompain[1,2,*]

ABSTRACT

The Golgi complex is responsible for processing and sorting of secretory cargos. Microtubules are known to accelerate the transport of proteins from the endoplasmic reticulum (ER) to the Golgi complex and from the Golgi to the plasma membrane. However, whether post-Golgi transport strictly requires microtubules is still unclear. Using the retention using selective hooks (RUSH) system to synchronize the trafficking of cargos, we show that anterograde transport of tumor necrosis factor (TNF) is strongly reduced without microtubules. We show that two populations of Golgi elements co-exist in these cells. A centrally located and giantin-positive Golgi complex that sustains trafficking, and newly formed peripheral Golgi mini-stacks that accumulate cargos in cells without microtubules. Using a genome-edited GFP–giantin cell line, we observe that the trafficking-competent Golgi population corresponds to the pre-existing population that was present before removal of microtubules. All Golgi elements support trafficking after long-term depletion of microtubules and after relocation of Golgi proteins to the ER after treatment with Brefeldin A. Our results demonstrate that functional maturation of Golgi elements is needed to ensure post-Golgi trafficking, and that microtubule-driven post-Golgi transport is not strictly required.

KEY WORDS: Intracellular trafficking, Microtubules, Golgi

INTRODUCTION

In animal cells, proteins to be transported to the cell surface enter the secretory pathway at the level of the endoplasmic reticulum (ER) after their synthesis. They leave the ER through the ER exit sites (ERES) spread throughout the cell toward the Golgi complex. Proteins are then extracted from the trans-Golgi network toward the cell surface in post-Golgi carriers. The Golgi complex ensures correct targeting of secretory cargos and their correct processing. The Golgi complex and the secretory pathway are closely connected to the microtubule network (de Forges et al., 2012). Direct connection of the dynactin, a regulatory factor of the dynein complex, with COPII-positive carriers at the level of the ERES (Watson et al., 2005) enables ER-to-Golgi transport of cargos along microtubules. Later in their journey, cargos are transported in post-Golgi carriers along microtubules by kinesins, plus-end-directed motors. In addition, microtubules are essential for the integrity of the Golgi complex (Sandoval et al., 1984). In interphase mammalian cells, the Golgi complex is composed of stacked flattened cisternae forming a long ribbon (Farquhar and Palade, 1981). A Golgi matrix surrounds the Golgi complex which is composed of large coiled coil proteins like giantin (also known as GOLGB1) or GM130 (also known as GOLGA2). The perinuclear localization of the Golgi complex, close to the centrosome, is mediated by microtubules and dynein (Corthesy-Theulaz et al., 1992; Ho et al., 1989). Upon disruption of the microtubule network, Golgi mini-stacks keep their internal polarity from cis to trans and are apposed to the ERES (Cole et al., 1996). This apposition allows normal ER-to-Golgi transport in the absence of microtubules. In addition, the Golgi complex, as an entire organelle or as mini-stacks, nucleates microtubules and thus, like the centrosome, also plays the role of a microtubule-organizing center (Chabin-Brion et al., 2001; Efimov et al., 2007). Consequently, compaction and clustering of dispersed Golgi elements restart quickly after repolymerization of microtubules, for example upon nocodazole wash-out. Despite this clear link between microtubules and Golgi complex dynamics, it is still unclear whether microtubules are indispensable for an efficient trafficking of cargos to the plasma membrane. This question was already assessed in the 1990s–2000s but discrepancy exists (Cole et al., 1996; Hirschberg et al., 1998; Parczyk et al., 1989; Presley et al., 1997; Rindler et al., 1987; Rogalski et al., 1984; Van De Moortele et al., 1993). It was well demonstrated by these studies that ER-to-Golgi transport occurs in the absence of microtubules and that formation of peripheral mini-stacks requires ER export.

The mechanisms of formation of Golgi elements in the absence of microtubules have thus been well studied. The question we addressed here is whether post-Golgi transport intermediates can be produced in the absence of microtubules. We monitored secretory cargos transport in normal and in microtubule-depletion conditions using the retention using selective hooks (RUSH) assay (Boncompain et al., 2012). We revealed the co-existence of distinct subpopulations of Golgi elements early after removal of microtubules and assessed their secretion capacity. Our results demonstrated that, although secretory cargos are blocked in newly formed mini-Golgi elements, microtubule-independent secretion occurs from the pre-existing mature Golgi complexes. Upon longer incubation time in the absence of microtubules, or by forcing relocation of proteins in mini-stacks, all Golgi elements support transport in the absence of microtubules. Taken together, this indicates that production of post-Golgi transport intermediates does not require microtubules and that functional maturation of Golgi mini-stacks is essential to support transport. This functional maturation is likely to be the crucial step that is responsible for the block in transport observed at early stages upon microtubule removal.

RESULTS

Anterograde transport of secretory cargos is strongly reduced in the absence of microtubules

To analyze the involvement of microtubules in the transport of secretory cargos we took advantage of the RUSH assay that we

[1]Institut Curie, Centre de Recherche, PSL research University, 75005 Paris, France. [2]CNRS UMR144, 75005 Paris, France. [3]UPMC, 75005 Paris, France.
*These authors contributed equally to this work

‡Author for correspondence (franck.perez@curie.fr)

F.P., 0000-0002-9129-9401

Received 4 March 2016; Accepted 8 July 2016

Journal of Cell Science (2016) 129, 3238-3250 doi:10.1242/jcs.188870

developed, which allows quantitative and real-time analysis of the secretory pathway. Briefly, reporter proteins fused to a streptavidin-binding peptide (SBP) are retained in the ER by an ER-resident protein fused to core streptavidin. Synchronous release of the cargo is achieved at physiological temperature using biotin (Boncompain et al., 2012). In this study, we focused our attention on the anterograde transport of tumor necrosis factor (TNF) and mannosidase II (ManII, also known as MAN2A1), which are efficiently synchronized using the RUSH assay (Boncompain et al., 2012) although other cargos were also analyzed. The importance of microtubules in post-Golgi transport is still unclear in the literature. Part of the discrepancy might be due to incomplete depolymerization of microtubules in certain studies. In the present study, we ensured complete removal of microtubules before release of the cargos from the ER by first incubating cells on ice for 90 min before warming them up in medium containing nocodazole for 30 min. This treatment ensures complete removal of microtubules whereas incubation with nocodazole alone keeps stable microtubules (Fig. S1A). In control cells, TNF–SBP–EGFP and ManII–SBP–mCherry reached the Golgi complex within 15 min after biotin addition and TNF–SBP–EGFP was expressed at the cell surface from 30 min (Fig. 1A; Movie 1). The amount of TNF at the plasma membrane was strongly reduced when microtubules were removed (Fig. 1B; Movie 2). Even after a longer time of trafficking, the level of TNF at the plasma membrane in the absence of microtubules was lower than in control cells as quantified by flow cytometry (Fig. 1C). The same phenotype was observed for VSVG (both the wild-type VSVG in the RUSH system and the thermosensitive mutant tsO45) (Fig. S1B,C) and for other cargos (data not shown). Thus, as described previously (Cole et al., 1996; Presley et al., 1997; Storrie et al., 1998), the absence of microtubules does not inhibit ER-to-Golgi transport. However, it strongly reduces trafficking of secretory cargos towards the plasma membrane.

Blockade of post-Golgi transport is not due to Golgi dispersion

Washout of nocodazole induces a fast re-polymerization of the microtubule network and subsequent re-clustering of Golgi elements and their centripetal movement (Ho et al., 1989). After washout of nocodazole, TNF reached the plasma membrane after exit from dispersed Golgi elements as observed by real-time imaging (Fig. 2A; Movie 3). Microtubule regrowth and post-Golgi trafficking occurred concomitantly with clustering and compaction of the Golgi elements at the cell center (Fig. 2B). The reasons why trafficking resumed from these dispersed Golgi elements as soon as microtubules regrew were unclear. It might be because of Golgi elements re-clustering and fusing because isolated Golgi elements might not be competent for trafficking (Glick and Luini, 2011; Pfeffer, 2010). We thus dispersed Golgi elements without removing microtubules and analyzed transport in these conditions. This was achieved by overexpressing a dominant-negative dynactin construct (p150-CC1) that perturbs dynein activity (Quintyne et al., 1999). As expected, in cells overexpressing p150-CC1, the Golgi complex was dispersed throughout the cell. However, TNF was normally transported to the plasma membrane (Fig. 3A,B). If nocodazole was added to p150-CC1 expressing cells, a Golgi block was observed (Fig. 3C,D). Nocodazole washout allowed transport of TNF to resume even in cells where Golgi elements remained dispersed due to overexpression of p150-CC1 (Fig. 3E). Thus, Golgi dispersion is not responsible per se for the Golgi block observed in the absence of microtubules.

Two populations of Golgi elements co-exist early after removal of microtubules

Golgi dispersion observed upon removal of microtubules is due to the formation of Golgi mini-stacks apposed to the ERES (Cole et al., 1996; Storrie et al., 1998). In the absence of microtubules, TNF released from the ER accumulated in dots colocalized with ManII and GM130 after 90 min of transport (Fig. S2A). Cryo-immunoelectron microscopy confirmed that, in this condition, TNF was accumulated in 'onion-shaped' Golgi mini-stacks positive for GM130 (Fig. 4A). In control conditions, in the presence of microtubules, TNF was detected in Golgi stacks after 15 min of trafficking but not after 90 min (Fig. S2B).

Surprisingly, careful examination of time-lapse imaging revealed that the block observed in nocodazole-treated cells was not complete. In microtubule-depleted cells, TNF reached the scattered Golgi elements homogenously within 15 min (linescans 1 and 2, Fig. 4B) and a fraction of TNF was then able to exit perinuclear Golgi elements (linescan 3, Fig. 4B) while another pool of TNF accumulated in peripheral mini-stacks (linescan 4, Fig. 4B; Movie 4). This was confirmed by cryo-immunoelectron microscopy as we observed, in the same cell, that some GM130-positive mini-stacks contained TNF whereas others did not (Fig. 4A). These results suggest that two functionally different populations of the Golgi complex coexist in cells after microtubule removal. We reported before that two pools of Golgi elements can be distinguished in cells using giantin as a distinguishing marker (Nizak et al., 2003). We also looked at the localization of proteins involved in nucleating microtubules at the Golgi complex. AKAP450 (also known as AKAP9) was detected on the Golgi complex and GFP–CLASP2 on Golgi and microtubules in control cells. In the absence of microtubules, AKAP450 and GFP–CLASP2 were observed on Golgi mini-stacks as previously described (Efimov et al., 2007; Rivero et al., 2009). AKAP450 and GFP–CLASP2 were less abundant on newly formed, peripheral Golgi mini-stacks, behaving like giantin (Fig. S3A,B).

We observed that TNF was able to leave the giantin-positive Golgi pool even in the presence of nocodazole, demonstrating the ability of the giantin-positive pool to perform secretion (Fig. 4C). To assess the dynamics of endogenous giantin, we developed a gene-edited GFP–giantin cell line using CRISPR-Cas9 technology (see Materials and Methods, Fig. S3C,D). All giantin alleles were tagged with GFP in the HeLa clone used in this study (GFP–giantin^{EN}). Dispersion of Golgi elements was imaged in real-time upon warming-up cells in nocodazole using the GFP–giantin^{EN} cell line. Giantin-positive Golgi elements remained compact and ManII–mCherry appeared quickly in newly formed peripheral mini-stacks (Fig. S3E). We confirmed that giantin-positive Golgi elements were found close to the centrosome in the absence of microtubules after seeding cells on micro-patterns to homogenize their shape (Fig. S3F,G). These results confirmed the coexistence of two populations of Golgi elements shortly after removal of microtubules. The giantin-positive population corresponds to the Golgi that was present before microtubule removal whereas newly formed mini-stacks were giantin-negative and appeared throughout the cell. Our results suggest that the giantin-positive Golgi elements are able to mediate secretion of cargos in the absence of microtubules.

The two populations of Golgi elements show different secretion ability

We then assessed the functional state of the two populations of Golgi elements. Upon removal of microtubules, not only was the

Journal of Cell Science (2016) 129, 3238-3250 doi:10.1242/jcs.188870

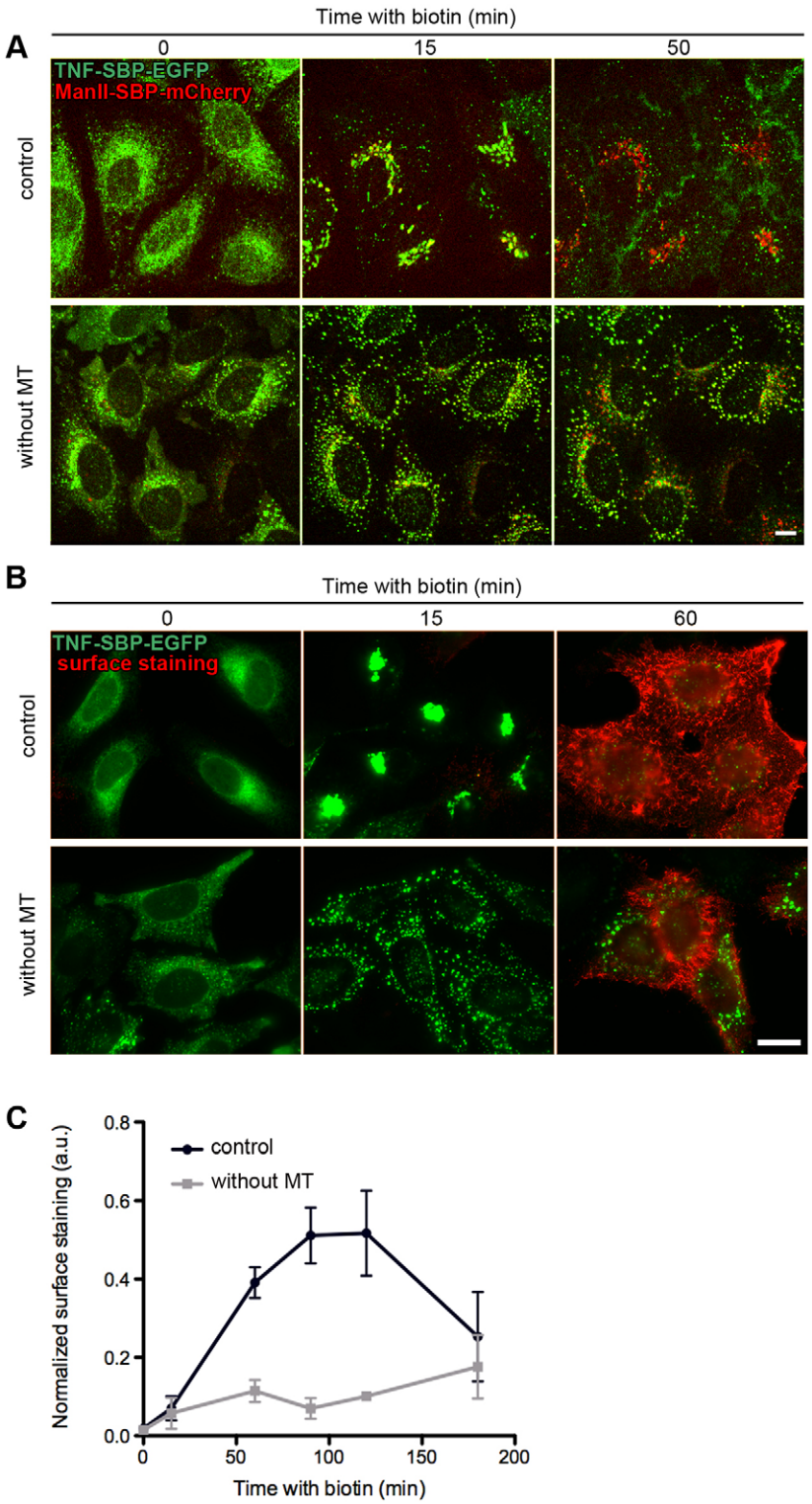

Fig. 1. TNF post-Golgi trafficking is strongly reduced in the absence of microtubules. HeLa cells stably expressing streptavidin (Str)–KDEL as a hook and TNF–SBP–EGFP and ManII–SBP–mCherry (A), or expressing Str–KDEL as a hook and TNF–SBP–EGFP only (B,C) were subjected to microtubule removal (without MT) or were treated with DMSO as a control. Induction of trafficking by addition of biotin was performed at time 0. (A) Cells were observed by time-lapse imaging using a spinning disk microscope and pictures were acquired at the indicated time. (B) Surface staining using an anti-GFP antibody (red) was performed on non-permeabilized cells at the indicated time after induction of TNF trafficking. (C) Quantification by flow cytometry of cells treated as in B. The mean±s.d. of three independent experiments is shown with more than 5000 cells per condition. a.u., arbitrary units. Scale bars: 10 µm.

quantity of TNF that reached the plasma membrane reduced but it was not homogenously distributed. A stronger surface staining was observed at the giantin-proximal side of the plasma membrane (Fig. 5A). To assess the secretion capability of the central Golgi complex, we performed inverse fluorescence recovery after photobleaching (iFRAP) experiments after microtubule removal. The quantification is shown in Fig. 5B. After 14 min of trafficking, when TNF is localized in all Golgi elements, the entire cell fluorescence was bleached (blue cell, Fig. 5B) except the area corresponding to the compact Golgi elements (area 3 in red, Fig. 5B). Time-lapse analysis showed that the fluorescence signal decreased in the compact Golgi complex (area 3, Fig. 5B). Signal increase at the plasma membrane could not be detected, probably because the intensity was too low. In the control non-bleached cell, fluorescence decreased at the side of the cell that we identified as the compact Golgi complex (area 1, Fig. 5B). At the other side of the

Journal of Cell Science (2016) 129, 3238-3250 doi:10.1242/jcs.188870

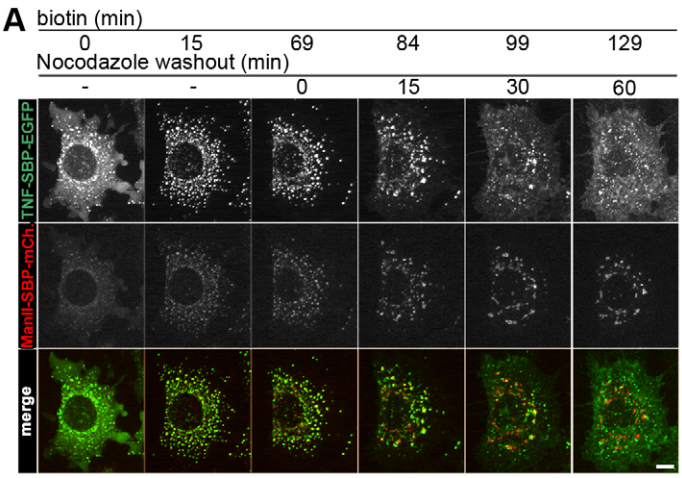

Fig. 2. TNF trafficking resumes upon microtubule regrowth and clustering of Golgi elements. (A) HeLa cells stably expressing streptavidin (Str)–KDEL, TNF–SBP–EGFP and ManII–SBP–mCherry were subjected to microtubule removal. Cells were observed by time-lapse imaging using a spinning disk microscope and pictures were acquired at the indicated time. Biotin was added at time 0. After 69 min of incubation with biotin, nocodazole was washed out. Scale bar: 10 µm. (B) Quantification of Golgi elements from the experiment shown in A before and 60 min after nocodazole washout.

cell, which corresponds to peripheral mini-stacks, fluorescence was kept at the same level showing that TNF accumulated and does not exit from these Golgi elements (area 2, Fig. 5B; Movie 5). iFRAP experiments thus confirmed the presence of two populations of Golgi elements with different trafficking ability. The compact giantin-positive pool of Golgi elements sustains TNF transport to the plasma membrane in the absence of microtubules. Transport carriers probably reach the plasma membrane by diffusion.

We also investigated the glycosylation capacity of the populations of Golgi elements. Lectins recognize with high specificity different types of sugars and sugar branching. They can be used as a marker of the glycosylation state of proteins. *Helix pomatia* agglutinin (HPA) binds to α-N-acetylgalactosamine, which is added to proteins in early Golgi compartment. Wheat germ agglutinin (WGA), which binds to N-acetylglucosamine and sialic acid, is commonly used as a marker of the trans-Golgi. HPA showed a differential staining between the two populations of Golgi elements in the absence of microtubules (Fig. 5C). The HPA signal was stronger in peripheral Golgi mini-stacks compared to central giantin-positive Golgi elements. In contrast, the distribution of WGA signal did not show obvious differences between control cells and cells without microtubules. These results show that proteins present in the Golgi when cells were fixed have a different glycosylation status. Golgi glycosylation enzymes responsible for the modifications probably relocalize to the peripheral Golgi elements with different kinetics, as previously described (Yang and Storrie, 1998). Enzymes responsible for the sugar branching detected by HPA might quickly relocalize to peripheral Golgi elements whereas those detected by WGA might stay longer in the compact Golgi. In the same line, we cannot rule out that additional glycosylation branching occurs in the compact Golgi that would prevent detection by HPA. In addition, cargo substrates for the different glycosylation enzymes might not accumulate in the compact Golgi given that it is competent for secretion.

Functional maturation of Golgi elements is required for secretion in the absence of microtubules

Why Golgi mini-stacks were incompetent for secretion was unclear. It is indeed intriguing to see that Golgi export can occur from the giantin-positive Golgi elements indicating that microtubules are not essential to drive cargo export from Golgi membranes. We reasoned that mini-stacks might be unable to sustain secretion because components present in giantin-positive Golgi complexes were missing in Golgi elements formed within 30 min of nocodazole treatment. To enable functional maturation of Golgi mini-stacks, cells were kept without microtubules overnight before inducing the trafficking of TNF. In this condition, TNF reached the plasma membrane to almost the same level as in control cells with microtubules (Fig. S4A,B). A similar result was obtained after 6 h of nocodazole pre-treatment. In these conditions, TNF transport to the plasma membrane reached ∼70% of that in the DMSO control whereas it reached only 15% after 30 min of nocodazole treatment (Fig. 6A,B). Interestingly, after a long treatment with nocodazole, Golgi elements were scattered throughout the cytoplasm and giantin was detected on all of them (Fig. S4A). These results suggest that mini-stacks formed in the absence of microtubules need time to become functional and to sustain cargo transport. We imaged in real-time the appearance of the two populations of Golgi elements after microtubule removal using fluorescently tagged giantin and ManII. Giantin gene-edited cells were transiently transfected with ManII–Cherry and were imaged during long-term nocodazole treatment. As expected, re-localization of Golgi enzymes to scattered dots was rapid, owing to fast recycling through the ER. In contrast, giantin-positive compartments remained more compact and centrally located for a longer time after microtubule removal (Fig. 6C). However, giantin was gradually enriched in dispersed Golgi mini-stacks and was clearly visible in these elements after 4 h of incubation with nocodazole. Thus, giantin, and probably other Golgi proteins, only slowly reach newly formed Golgi mini-stacks in the absence of microtubules. We showed that the slow appearance of giantin in peripheral mini-stacks is mediated by relocation of pre-existing giantin from older Golgi elements and not by newly synthesized protein. We pre-treated cells with cycloheximide to inhibit protein synthesis and confirmed, by use of a SUnSET assay (Schmidt et al., 2009), that strong inhibition was still observed after 8 h of treatment (see Materials and Methods). Even in these conditions, giantin relocalized to peripheral Golgi elements in the absence of microtubules, demonstrating that its late appearance on mini-stacks is due to slow recycling (Fig. 7A,B).

This slow functional maturation is responsible for the lack of transport at early time points after microtubule removal. Although the missing factors on newly formed Golgi mini-stacks were still unknown, giantin was an attractive candidate. In one set of experiments, we forced giantin to be present on all mini-stacks at early time points by overexpressing giantin, but this did not allow TNF to be efficiently exported from mini-stacks in the absence of microtubules (Fig. S4C). In another set of experiments, we depleted giantin by using small interfering RNA (siRNA) to test its

Journal of Cell Science (2016) 129, 3238-3250 doi:10.1242/jcs.188870

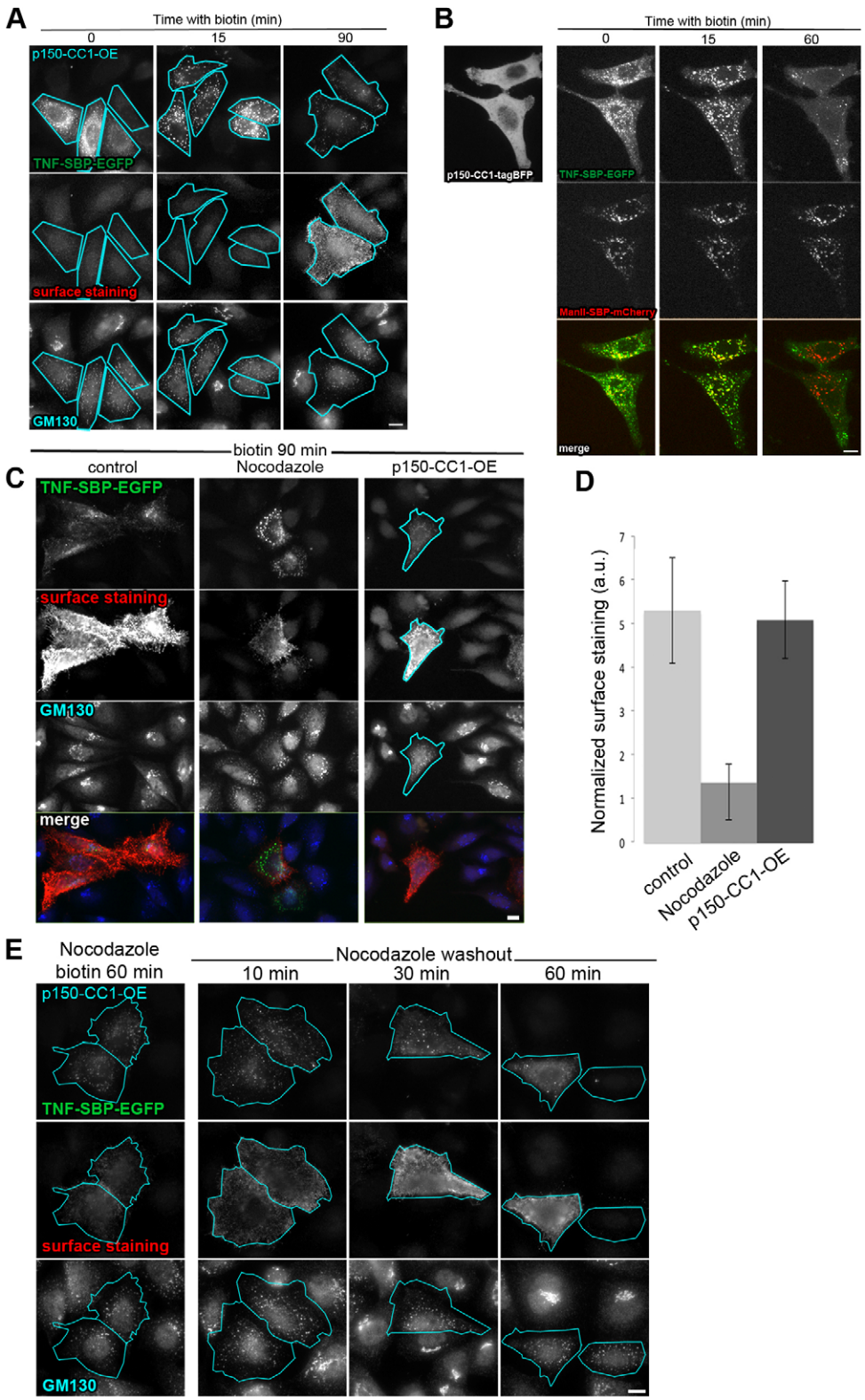

Fig. 3. The lack of post-Golgi transport is not due to Golgi dispersion. (A) HeLa cells transfected with streptavidin (Str)–KDEL_TNF–SBP–EGFP and p150-CC1–tagBFP. Cells expressing p150-CC1–tagBFP are outlined in blue. Surface staining of TNF was detected with an anti-GFP antibody on non-permeabilized cells. The Golgi complex was counterstained with an anti-GM130 antibody. Biotin was added at time 0. (B) HeLa cells transfected with Str–KDEL_TNF–SBP–EGFP, Str–KDEL_ManII–SBP–mCherry and p150-CC1–tagBFP. Real-time pictures were acquired with a spinning disk microscope. Biotin was added at time 0. (C) HeLa cells transfected with Str–KDEL_TNF–SBP–EGFP with or without p150-CC1–tagBFP were subjected to cold and DMSO (control) or nocodazole treatments. Cells overexpressing p150-CC1–tagBFP (p150-CC1-OE) are outlined in blue. Surface detection of TNF–SBP–EGFP was performed using an anti-GFP antibody (red). The Golgi complex was counterstained with an anti-GM130 antibody (blue). (D) Quantification of the surface staining (mean±s.d.) was achieved using the Icy software (see Materials and Methods). At least 35 cells were quantified per condition. (E) HeLa cells transfected with Str–KDEL_TNF–SBP–EGFP and p150-CC1–tagBFP were subjected to microtubule removal. Cells overexpressing (OE) p150-CC1–tagBFP are outlined in blue. Washout of nocodazole was performed after 60 min of incubation with biotin. Surface detection and Golgi staining were performed as in C. Scale bars: 10 µm.

involvement in the functional maturation of Golgi mini-stacks. Even though giantin was strongly depleted, TNF reached the plasma membrane with the same rate as in cells transfected with control siRNA (Fig. S4D,E). These results suggest that other factors might be missing on newly formed mini-stacks.

Because slow recycling from older Golgi elements to newly formed mini-stacks seems to be responsible for transport block in the absence of microtubules, we sought to artificially accelerate functional maturation of mini-stacks. We pre-treated cells with Brefeldin A (BFA) before removing microtubules to accumulate most Golgi proteins in the ER. Then BFA was washed out in the presence of nocodazole to form mini-stacks that should contain the majority of Golgi proteins, without the need for slow recycling; for example, in these conditions, giantin was detected on all Golgi

Journal of Cell Science (2016) 129, 3238-3250 doi:10.1242/jcs.188870

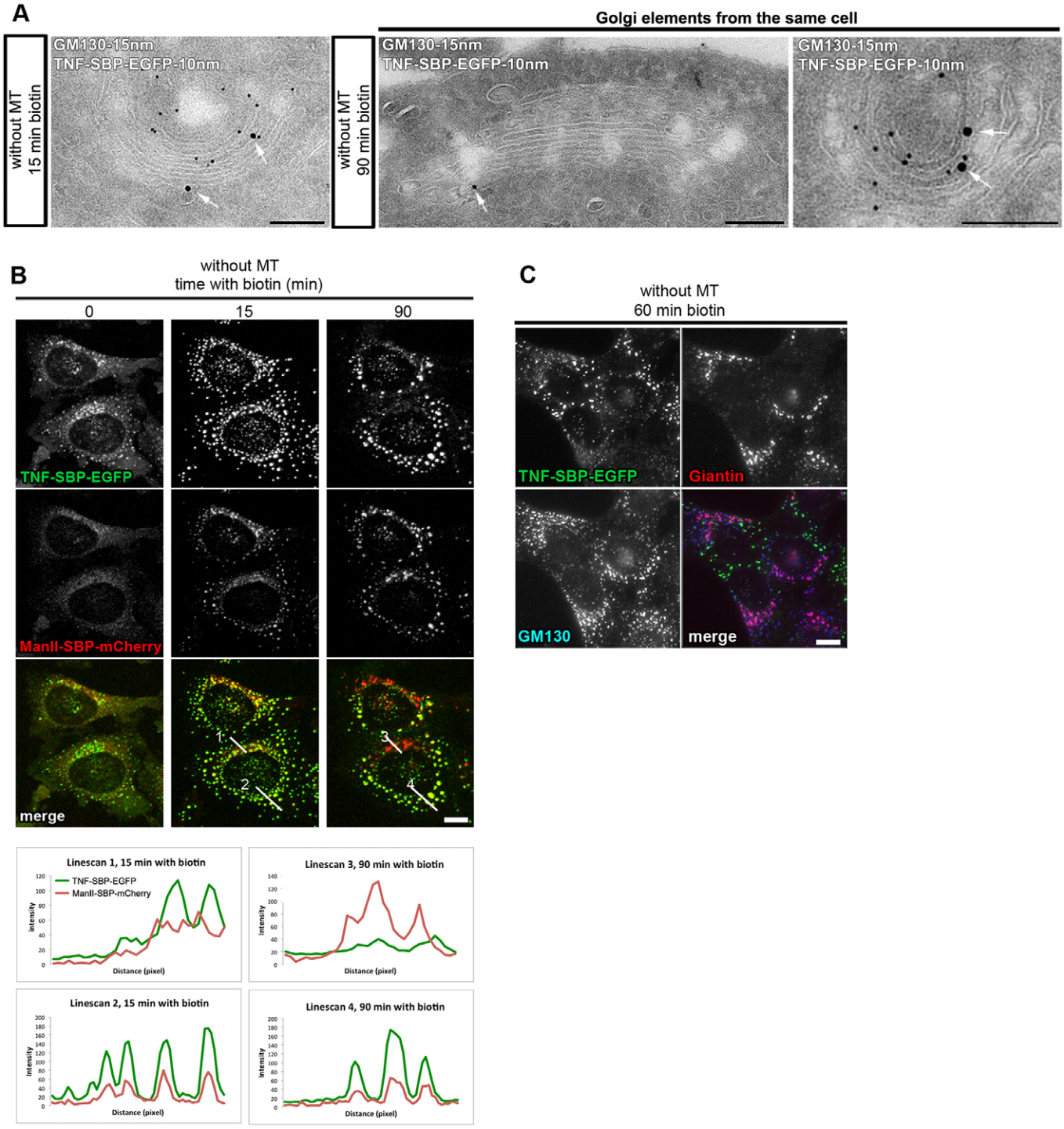

Fig. 4. Two populations of Golgi complex coexist shortly after removal of microtubules. (A) Cryo-immunoelectron microscopy performed on HeLa cells stably expressing streptavidin (Str)–KDEL_TNF–SBP–EGFP after microtubule removal (without MT). TNF–SBP–EGFP was labeled with an anti-GFP antibody and the Golgi complex with an anti-GM130 antibody. TNF is detected with 10 nm PAG (Protein-A-conjugated gold) and GM130 with 15 nm PAG (arrows). Scale bars: 200 nm. (B) HeLa cells stably expressing Str–KDEL and TNF–SBP–EGFP and ManII–SBP–mCherry after microtubule removal. Cells were observed by time-lapse imaging using a spinning disk microscope and pictures were acquired at the indicated time. Biotin is added at time 0. Intensity profiles were obtained with Metamorph software on the indicated lines. Scale bar: 10 µm. (C) HeLa cells stably expressing Str–KDEL_TNF–SBP–EGFP after microtubule removal and after 60 min of addition of biotin. Immunostaining using anti-GM130 (blue) and anti-giantin (red) antibodies was performed. Scale bar: 10 µm.

mini-stacks (Fig. S4F). These mini-stacks were functional and sustained transport. TNF released from the ER in these conditions was able to traffic to the plasma membrane at a level similar to microtubule-containing control cells (Fig. 7C,D). This suggests that Golgi-to-ER recycling is the limiting factor for functional maturation, and not Golgi dispersion per se. Accordingly, rapid dispersion of Golgi elements, without affecting Golgi-to-ER recycling should not inhibit secretion. To test this hypothesis, dynein activity was rapidly inhibited by acute expression of p150-CC1 using a cycloheximide wash-out protocol to accumulate

Journal of Cell Science (2016) 129, 3238-3250 doi:10.1242/jcs.188870

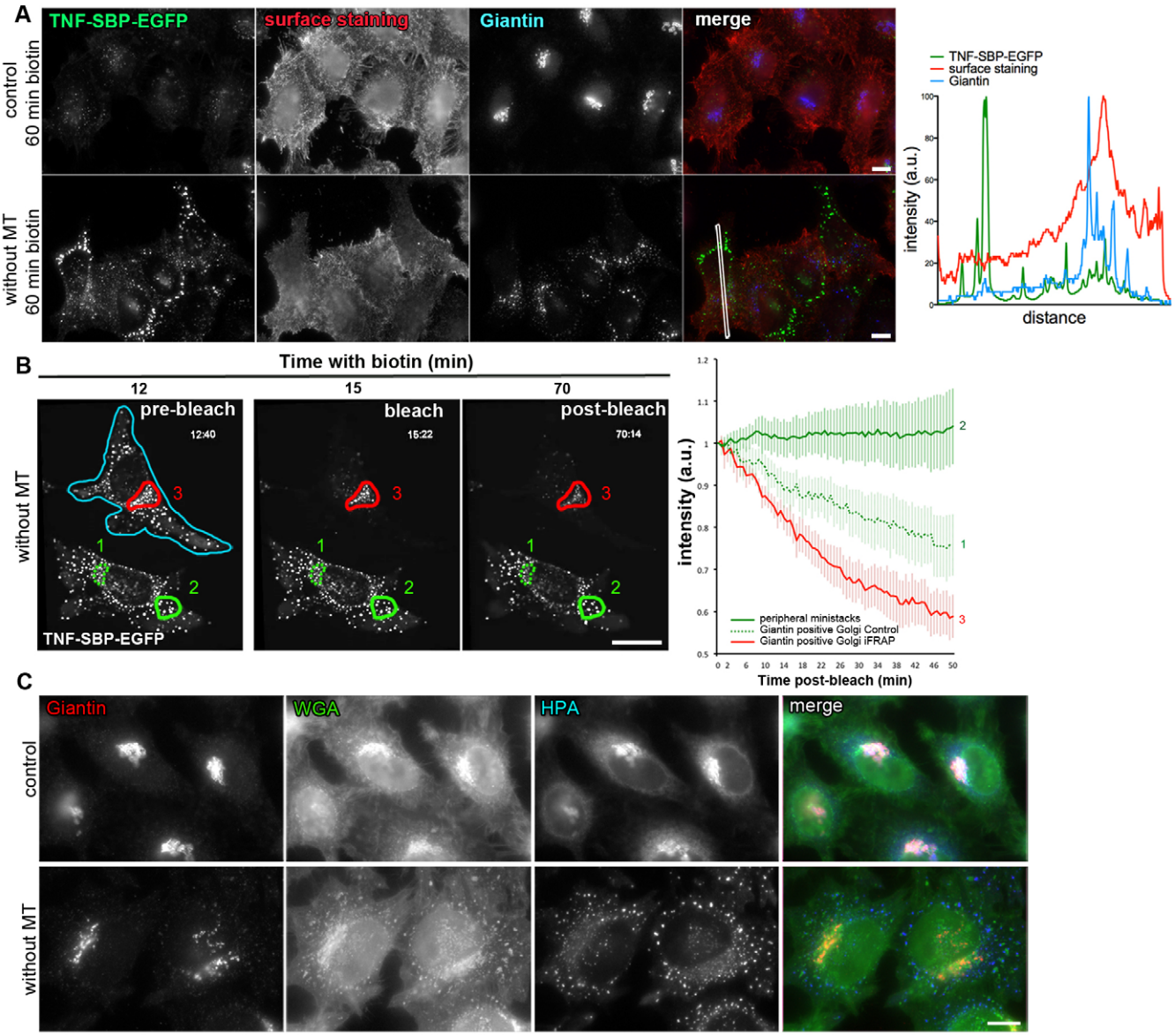

Fig. 5. The two populations of Golgi elements are functionally different. (A) HeLa cells stably expressing streptavidin (Str)–KDEL_TNF–SBP–EGFP were subjected to microtubule removal (without MT). Surface staining was performed using an anti-GFP antibody (red) on non-permeabilized cells. The Golgi complex was then counterstained with an anti-giantin antibody (blue). An intensity profile was obtained with the Metamorph software along the indicated line. (B) HeLa cells stably expressing Str–KDEL_TNF–SBP–EGFP were subjected to microtubule removal and treated with biotin at 37°C. Cells were observed by time-lapse imaging using a spinning disk microscope. After 14 min of incubation with biotin, fluorescence in the cell outlined in blue was photobleached except for the central Golgi complex area outlined in red. Fluorescence intensity was measured in the areas 1–3 indicated on the left panel in five independent experiments (area 1, *n*=10; area 2, *n*=16; area 3, *n*=7) and is presented as the is mean±s.d. (C) Immunostaining using fluorescent HPA (blue), fluorescent WGA (green) and an anti-giantin antibody (red) was performed on HeLa cells after microtubule removal or treatment with DMSO as a control. Scale bars: 10 µm.

p150-CC1 mRNA and pulse its expression for a short time (see Materials and Methods). A pulse of 2 h of was long enough to induce Golgi dispersion (Fig. 7E). In this condition, TNF trafficking was induced by addition of biotin. TNF transport at the plasma membrane was slightly decreased but much less so than in the absence of microtubules (Fig. 7F). This demonstrates that the block observed in the absence of microtubules is due to defects in functional maturation, mostly based on recycling through the ER, and not to a direct role of microtubules in export from the Golgi. In the condition of the rapid dynein inhibition, microtubules are still present and kinesin-dependent Golgi-to-ER transport is active whereas it is inhibited in the absence of microtubules. When dispersed, mini-stacks are functionally mature, upon long nocodazole incubation time or upon BFA washout, then microtubules are dispensable for Golgi-to-plasma membrane transport. This indicates that microtubule-driven transport is not strictly required for secretion of cargos in mammalian cells.

A natural stage where functional maturation of Golgi complexes might be particularly important is mitotic exit. It is known for decades that the Golgi complex disassembles during mitosis (Lucocq and Warren, 1987; Shima et al., 1998) and that anterograde transport is arrested. During mitosis, Golgi-to-ER transport is still efficient. It has been shown that Golgi enzymes, for instance, relocate to the ER during mitosis (Sengupta et al., 2015). Using the GFP–giantin^{EN} cell line and an antibody directed to GM130, we observed the behavior of these two Golgi matrix

Journal of Cell Science (2016) 129, 3238-3250 doi:10.1242/jcs.188870

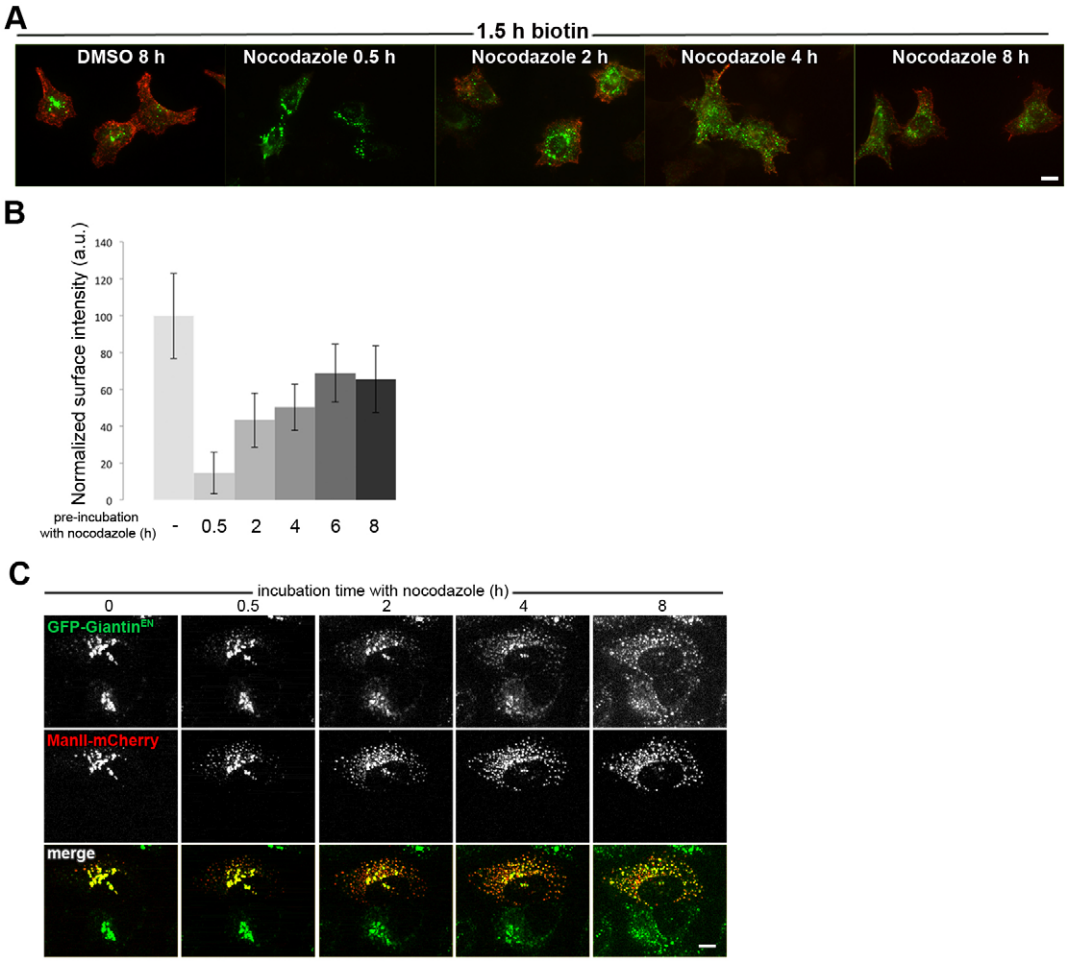

Fig. 6. Golgi mini-stacks need time to become functional after microtubule removal. (A) After a cold treatment, HeLa cells stably expressing streptavidin (Str)–KDEL and TNF–SBP–EGFP were incubated with nocodazole for the indicated time (0, 5, 2, 4, 6 or 8 h). Surface staining was performed using an anti-GFP antibody (red) on non-permeabilized cells. (B) Quantification (mean±s.d.) of the surface staining (37 to 97 cells were quantified depending on the condition from two independent experiments). (C) HeLa cells stably expressing endogenous giantin tagged with GFP (GFP–giantin^{EN}) transfected with ManII–mCherry were subjected to a cold treatment. Pictures were acquired with a spinning disk microscope right after the addition of nocodazole in the medium at 37°C to observe Golgi complex dispersion. Scale bars: 10 µm.

proteins during mitosis. As previously demonstrated, the Golgi complex disassembles in metaphase, with giantin and GM130 being scattered into multiple tiny dots (Fig. 8A). Careful examination showed that giantin and GM130 displayed distinct behavior. GM130-positive structures still showed the dot-like localization in metaphase and early anaphase, whereas giantin became completely diffuse. No visible giantin-positive structures were distinguishable. In late anaphase, Golgi elements became clearly giantin and GM10 positive, concomitantly with their clustering. According to our model, anterograde trafficking should resume at the step when giantin is present on Golgi mini-stacks. To assess this question, we imaged living cells stably expressing TNF–SBP–EGFP and ManII–SBP–mCherry. DNA was stained using SiR-DNA, to evaluate mitotic stage. Biotin was added when the cells were in metaphase. Post-Golgi transport of TNF resumed during late anaphase (Fig. 8B), which is the stage where giantin was clearly detected on Golgi elements in fixed samples. One can note that in the interphase surrounding cell, post-Golgi TNF transport occurred earlier than in the mitotic cell. These results suggest that upon mitosis exit, post-Golgi trafficking resumes when functional maturation of Golgi elements occurred, which is similar to what was observed in the absence of microtubules.

DISCUSSION

Role of microtubules in Golgi-dependent transport

Microtubules are essential for organizing and connecting intracellular compartments (de Forges et al., 2012). However, despite many studies, the role of microtubules in controlling Golgi-dependent transport is still unclear (Cole et al., 1996; Hirschberg et al., 1998; Parczyk et al., 1989; Presley et al., 1997; Rindler et al., 1987; Rogalski et al., 1984; Van De Moortele et al., 1993). Combining the RUSH assay with a complete removal of microtubules, we show here that, early after microtubule depletion, a large fraction of cargo is blocked in newly formed peripheral Golgi mini-stacks. The same result was also observed using the classic VSVG tsO45 assay.

Why transport is blocked in the absence of microtubules is unclear. One possibility was that dispersed mini-stacks are incompetent for transport. However, we show here that the dispersed state of mini-Golgi stacks is not directly responsible for the observed block because dispersion of the Golgi complex upon inhibition of dynein function did not perturb secretion. This is in line with a study by Yadav et al. (2009) who reported that secretion is not affected by dispersion of Golgi elements mediated by depletion of some golgins. Golgi size and integrity might be more

Journal of Cell Science (2016) 129, 3238-3250 doi:10.1242/jcs.188870

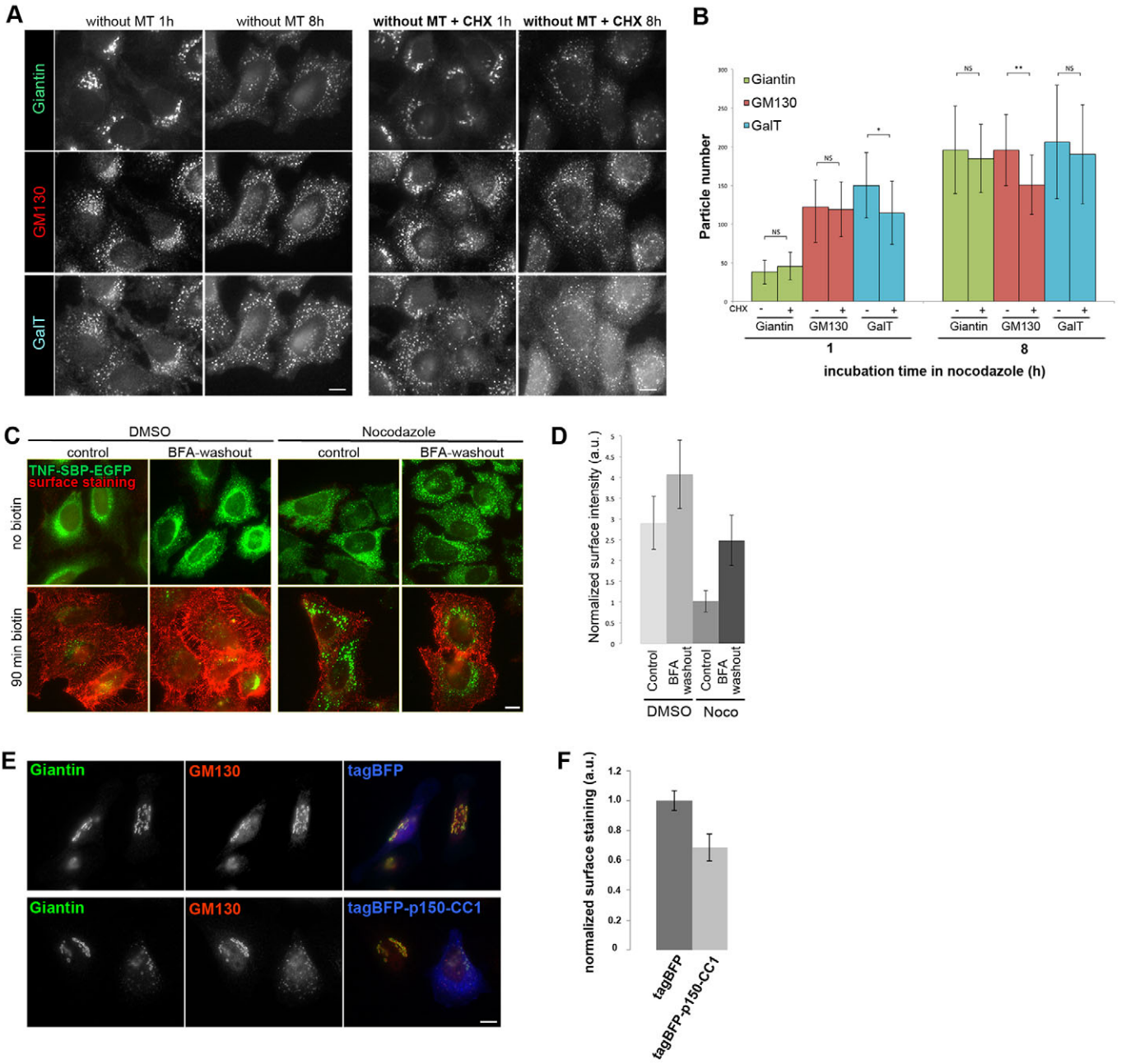

Fig. 7. Recycling of Golgi factors is sufficient for functional maturation of Golgi elements. (A) HeLa cells gene-edited to express endogenous giantin tagged with EGFP (GFP–giantin^{EN}) are subjected to cold and nocodazole treatments (without MT) in presence or in the absence of cycloheximide (CHX). Cells were fixed after 1 h or 8 h of treatments. The Golgi complex elements were stained with anti-GM130 (red) and anti-GalT (blue) antibodies. (B) Quantification (mean±s.d.) of Golgi elements (at least 45 cells from two independent experiments per condition). (C) HeLa cells stably expressing streptavidin (Str)–KDEL and TNF–SBP–EGFP were subjected to cold and DMSO or nocodazole treatments. When indicated, a BFA treatment followed by a washout of BFA (BFA-washout) was performed before the cold treatment. Surface staining was performed using an anti-GFP antibody (red) on non-permeabilized cells. (D) Quantification (mean±s.d.) of the surface staining (more than 50 cells were quantified per condition). (E,F) HeLa cells were subjected to acute expression of tagBFP–p150-CC1 or tagBFP as a control (blue). (E) The Golgi complex was stained with anti-giantin (green) and anti-GM130 antibodies (red). (F) TNF trafficking at the plasma membrane was quantified (mean±s.d., two independent experiments.) after staining with an anti-GFP antibody on non-permeabilized cells. Scale bars: 10 µm.

important for particular cargos, such as large cargos as recently suggested (Ferraro et al., 2014; Lavieu et al., 2014).

A second possibility was that microtubules, and their associated kinesin motors, were essential to enable export from Golgi or trans-Golgi network. However, we showed here that microtubule-driven mechanisms are dispensable for Golgi export. First, we observed that older, centrally localized and giantin-positive Golgi complexes support transport in the absence of microtubules. Second, we observed that after an extended period of time in the presence of nocodazole, cells are able to transport secretory cargo normally toward the plasma membrane. Third, cargos were able to leave dispersed mini-Golgi elements produced in a BFA washout experiment in the absence of microtubules. Taken together, this indicates that neither the overall size of Golgi mini-stacks, nor the need for motor-driven export from Golgi membranes are responsible for inhibition of transport observed at early time points

Journal of Cell Science (2016) 129, 3238-3250 doi:10.1242/jcs.188870

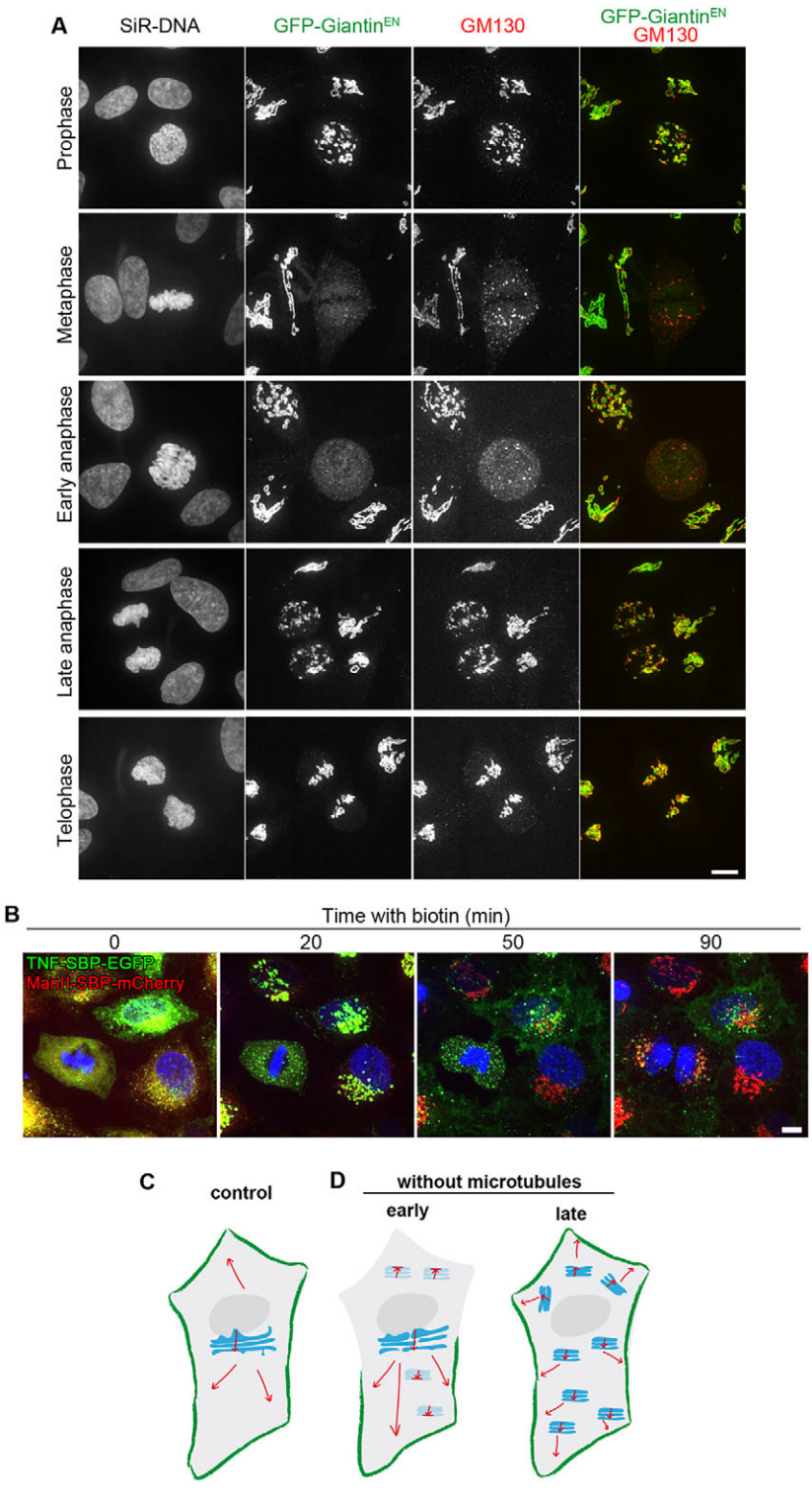

Fig. 8. Post-Golgi trafficking resumes at the time that Golgi elements become giantin-positive during mitosis. (A) HeLa cells expressing endogenous giantin tagged with GFP (GFP–giantin^{EN}, green) were fixed and stained for DNA (SiR-DNA) and GM130 (red). (B) HeLa cells stably expressing streptavidin (Str)–KDEL and TNF–SBP–EGFP and ManII–SBP–mCherry were imaged in real time. DNA was labeled with SiR-DNA to monitor the mitotic stage. Biotin was added when the cell was in metaphase. (C,D) Model for secretion in presence of microtubules (C), shortly (early) after removal of microtubules (D) and after long-term (late) removal of microtubules when mini-stacks are functionally mature. Scale bars: 10 µm.

in the absence of microtubules. We propose that functional maturation is necessary to enable Golgi transport (see below) and this might also be at work during mitosis exit.

In the absence of microtubules, it is likely that movement of transport intermediates toward the cell surface occurs by diffusion. This is suggested by the fact that secretion occurs in a Golgi proximal area of the plasma membrane when partial transport occurs exclusively from older giantin-positive Golgi elements upon short nocodazole treatment. Similar results were obtained by Schmoranzer et al. (2003) when they reported that fusion of exocytotic vesicles was clustered around central Golgi elements in the absence of microtubules. Thus, although microtubules are often described as essential to support polarized trafficking to sub-domains of the plasma membrane, we show here that, conversely, they are also essential to support homogenous transport to the cell surface when a unique central Golgi is present, because they support long-range transport (Fig. 8C). This is different in specialized cells as it has been well established that very long range and polarized

Journal of Cell Science (2016) 129, 3238-3250 doi:10.1242/jcs.188870

transport depend on microtubules (Conde and Caceres, 2009; Sugioka and Sawa, 2012).

Functional maturation of Golgi mini-stacks

Our data thus suggest that neither the small size of mini-stacks nor the obligatory use of microtubule-based motors are likely to explain the block in transport observed at early time points in the absence of microtubules. As an alternative model to explain why cargos cannot cross Golgi mini-stacks in these conditions, we propose that functional maturation of Golgi elements is essential to make them competent for secretion.

Soon after microtubule depletion, transport can only occur through a fully mature Golgi complex that existed prior to depletion (Fig. 8D, early). At a later stage, upon long nocodazole treatment, all mini-stacks become functionally mature and competent for transport (Fig. 8D, late). Experiments done in the presence of cycloheximide suggested that functional maturation of newly formed Golgi elements mostly occurs by the recycling of key factors from older Golgi complexes. Golgi dispersion throughout the cytoplasm after depolymerization of microtubules does not result from unlinking of the Golgi ribbon but to the appearance of Golgi mini-stacks at peripheral sites. It has been clearly demonstrated that mini-stacks are formed at ERES from recycling of Golgi proteins through the ER (Cole et al., 1996; Sengupta et al., 2015; Storrie et al., 1998). In addition, removal of microtubules does not prevent retrograde transport of Golgi proteins to the ER. This was well demonstrated by preventing ER export (using BFA or H89, or dominant-negative Sar1) at the same time as microtubule disruption (Jiang et al., 2006; Puri and Linstedt, 2003; Storrie et al., 1998). In our study, inhibiting new synthesis of proteins did not prevent functional maturation of Golgi elements. After several hours of incubation with nocodazole and cycloheximide, giantin, a marker of the pre-existing central Golgi, relocalized to peripheral mini-stacks. In the same line, forcing the recycling of Golgi proteins through the ER before removal of microtubules induced a full maturation of dispersed Golgi elements. In this condition, all newly formed mini-stacks were competent for secretion.

The missing components in immature mini-stacks

It is still unclear what are the Golgi factors needed to get functionally mature Golgi elements. We observed that Golgi enzymes might be only partly relocalized to new mini-stacks at early time points. Indeed, we showed a differential staining pattern with the lectin HPA between the central Golgi and peripheral mini-stacks. WGA staining was homogenously distributed to all Golgi elements, including central and peripheral elements. This might be due to different rates of relocalization of Golgi enzymes to peripheral mini-stacks after microtubule depolymerization as reported before (Yang and Storrie, 1998) and a functional glycosylation machinery might be essential to enable normal Golgi transport. However, this might also be due to the observed differential post-Golgi trafficking ability of the two populations of Golgi elements, given that cargos (glycosylation substrates) do not accumulate in the central Golgi elements.

The prominent Golgi proteins missing in immature mini-stacks is giantin and it is thus tempting to consider it as a key maturation factor. We show here that relocation of giantin to peripheral mini-stacks upon removal of microtubules takes several hours. This might be explained by slow dynamics, in particular slow ER recycling of this very large protein. In contrast, GM130 or Golgi enzymes are quickly relocalized on newly formed mini-Golgi. However, we have reported before that other proteins, like dymeclin (Dimitrov et al., 2009), are also localized on old and centrally localized Golgi elements shortly after nocodazole treatment, indicating that giantin is not the only Golgi protein to be retained on older Golgi structures. We observed that forced localization of giantin on all mini-stacks did not render them competent for secretion in the absence of microtubules. In addition, post-Golgi transport of cells depleted from giantin still occurs normally. This indicates that giantin is not the only missing factor responsible for functional maturation of Golgi elements.

In conclusion, we show here that transport is blocked in cells depleted of microtubules but that this block is not due to the role of microtubule-dependent export from the Golgi but rather to a slow functional maturation of re-forming mini-Golgi. It will now be important to look for the key factors that are missing in early mini-stacks and that are essential for the Golgi complex to become functionally mature.

MATERIALS AND METHODS

Cells, plasmids and transfection

HeLa wild-type cells and GFP–giantin gene-edited cells were grown at 37°C with 5% CO_2 in Dulbecco's Modified Eagle's medium (DMEM; high glucose, GlutaMAX, LifeTechnologies) supplemented with 10% fetal calf serum (FCS; GE Healthcare), pyruvate sodium 1 mM (Life Technologies), penicillin and streptomycin (Life Technologies). HeLa cells stably expressing RUSH constructs were cultured as described previously supplemented with 4 µg/ml of puromycin (Invivogen). Cells were transfected with calcium phosphate 24 to 48 h before observation (Jordan et al., 1996). The HeLa GFP–giantin cell line was obtained using the CRISPR-Cas9 technology. A guide RNA (gRNA) targeting the ATG region (5′-GAAATGCTGAGCCGATTATC-3′) of the *GOLGB1* gene coding for giantin was constructed. This gRNA was co-transfected with Cas9, a donor DNA coding for GFP–giantin with 1 kb left and right homology arms. The positive cells were enriched by two consecutive sorting steps and cloned. The clone used in this study contains only edited alleles. For immunoblots, giantin was probed with polyclonal anti-giantin antibody (1:10,000, cat. no. PRB-114C, Covance) and a polyclonal anti-GFP antibody (1:10,000) obtained from the recombinant antibody platform of the Institut Curie. RUSH plasmids (available from Addgene) and ManII–mCherry were constructed as previously described (Boncompain et al., 2012). The RUSH stable cell lines expressing the ER hook streptavidin (Str)–KDEL and TNF–SBP–EGFP, Str–KDEL and ManII–SBP–mCherry were established using lentiviral transduction. VSVGtsO45–EGFP was obtained from Jamie White (EMBL, Heidelberg, Germany). p150-CC1-BFP was constructed from p150-CC1–GFP given by Stéphanie Miserey-Lenkei (Institut Curie, Paris, France). Plasmid coding for GFP–CLASP2 was given by Anna Akhmanova (Utrecht University, The Netherlands). The siRNA sequence to target giantin was 5′-GAAGGUCUGUGAUACUCUA-3′. The control siRNA targeting luciferase was 5′-CGUACGCGGAAUACUUCGA-3′. siRNA were transfected with Lipofectamine RNAi MAX (Thermo Scientific) at 14-.5 nM for 72 h and a second transfection was performed in the same conditions for 48 h to ensure efficient depletion of giantin.

Acute expression of p150-CC1

HeLa cells were transfected with a plasmid encoding for tagBFP–p150-CC1 and Str–KDEL_TNF–SBP–EGFP or with tagBFP and Str–KDEL_TNF–SBP–EGFP as a control using calcium phosphate transfection (see above). After 3 h of transfection, cycloheximide (Sigma) was added at 0.1 mg/ml final concentration and incubated overnight to accumulate mRNA. Then cycloheximide was extensively washed out to allow protein synthesis. Incubation in the absence of cycloheximide was performed for 2 h before induction of trafficking by addition of biotin.

Treatments

Depolymerization of microtubules was performed with a cold treatment in HBSS (Life Technologies) at 4°C for 1.5 h. Cells were then warmed up in complete medium containing either nocodazole at 10 µM final

concentration or DMSO as control for 30 min at 37°C. Synchronization of the trafficking with the RUSH system was induced by addition of 40 µM final concentration biotin as described previously (Boncompain et al., 2012). Cycloheximide (Sigma-Aldrich) was used at 10 µg/ml. The efficacy of cycloheximide treatment was confirmed using the SUnSET assay (Schmidt et al., 2009). Cells were incubated with puromycin for 30 min before the end of cycloheximide treatment. Protein synthesis was monitored by detection of puromycin incorporation by western blotting using an anti-puromycin antibody (1:10,000, cat. no. MABE343, clone 12D10, Millipore). In these conditions, we confirmed efficient inhibition of translation at up to 8 h of treatment. Brefeldin A was used at 1 µM final concentration. Washout of nocodazole was performed by three washes with complete medium and washout of Brefeldin A was performed with ten washes. All molecules were purchased from Sigma-Aldrich.

Immunofluorescence, antibodies and microscopy

Cells fixation was performed with 3% paraformaldehyde (Electron Microscopy Sciences) for 15 min at room temperature or with methanol for 5 min at −20°C. For permeabilization, cells were incubated in PBS supplemented with BSA and saponin for 10 min at room temperature. The surface staining was performed at 4°C on non-fixed cells, the primary antibody was incubated in cold PBS for 40 min. Cells were then fixed with 2% paraformaldehyde for 10 min at room temperature. Primary antibodies used in this study are anti-GFP (Roche, cat. no. 11814460001, batch 11063100, dilution 1:1000), mouse anti-GM130 from BD Bioscience (cat. no. 610823, batch 4324839, dilution 1:1000), rabbit anti-GM130 from Abcam (cat. no. ab52649, batch GR147765-1, dilution 1:2000), anti-GalT from CellMAB (cat. no. CB02, batch 001, dilution 1:100) and anti-giantin TA10 (Nizak et al., 2004) antibodies, as well as an antibody directed against the lumenal domain of VSVG (anti-VG) (from Thomas Kreis, University of Geneva, Switzerland). Anti-ninein 1H2 (A-R-H-29, dilution 1:200), anti-β-tubulin S11B (A-R-H-23, dilution 1:25), anti-giantin TA10 (A-R-H-03, dilution 1:250) and anti-Cherry (A-P-R#13 dilution 1:1000) antibodies were obtained from the recombinant antibody platform of the Institut Curie, Paris, France. HPA and WGA lectins were purchased from Life Technologies (Thermo Scientific). Conjugated secondary antibodies were purchased from Jackson Immunoresearch. SiR-DNA was purchased from Spirochrome. Fixed pictures were acquired with an epifluorescence microscope (Leica) equipped with a Coolsnap camera (Roper Scientific). Time-lapse acquisitions were performed at 37°C in a thermostat-controlled chamber using an Eclipse 80i microscope (Nikon) equipped with a spinning disk confocal head (Perkin) and a Ultra897 iXon camera (Andor). Cells were incubated in Leibovitz's medium (Life Technologies) with or without drugs. FRAP experiments were performed on the same type of spinning disk microscope but equipped with a FRAP laser and a cool-SNAP HQ2 camera (Roper Scientific). The area of interest is bleached with a 405-nm laser (40× repetitions) 15 min after the addition of biotin. Image acquisitions in real time or on fixed samples were performed using Metamorph software (Molecular Devices).

Quantification of microscopy pictures

For Figs 2B and 7B, the number of Golgi complexes was quantified with the 'Analyze Particles' plugin of the ImageJ. For Fig. 3D, the surface staining performed by immunofluorescence was quantified using the Icy software after drawing the regions of interest corresponding to cells. Background average intensity was subtracted from the average intensity of the surface staining and normalized to the GFP expression level from which background was also subtracted. For Figs 6B, 8B, Figs S1C and S4B, the arrival at the plasma membrane was quantified using the average intensity of the anti-GFP antibody surface staining normalized to the GFP signal. The number of cells quantified for each experiment is indicated in the figure legends. For Fig. S3C, the distance was calculated between the centrosome (ninein staining) and each Golgi dot (GM130 or giantin positive) using x and y coordinates. The mean distance was calculated for each cell and then for each condition.

Flow cytometry

Cold treatment (HBSS, 4°C, 1 h 30 min) and nocodazole treatment (10 µM, 37°C, 30 min) were performed on HeLa cells on dishes as described above. Cells were detached with 0.5 mM EDTA and pelleted by centrifugation at 4°C for 5 min. Immunostaining was performed on ice. The primary antibody was incubated during 45 min on ice. Cells were post-fixed with paraformaldehyde 2% after incubation with the primary antibody and the washes with PBS containing BSA. The conjugated secondary antibody was incubated at room temperature for 30 min. Data were acquired with an Accuri C6 flow cytometer. The median intensity of the anti-GFP surface staining (FL4 channel) was divided by the median intensity of the GFP signal (FL1 channel) for each time point. These numbers were multiplied by 100 to express percentages.

Cryo-immunoelectron microscopy

Cells were fixed with 2% paraformaldehyde and 0.2% glutaraldehyde in 0.1 M sodium phosphate buffer, pH 7.4. After washing in PBS with 0.02 M glycine, cells were pelleted by centrifugation, embedded in 12% gelatin, cooled in ice and cut into 5-mm^3 blocks. The blocks were infused overnight with 2.3 M sucrose at 4°C, frozen in liquid nitrogen and stored until cryo-ultramicrotomy. Sections of 80 nm were cut with a diamond knife (Diatome) at −112°C using a Leica EM-UC7. Ultrathin sections were placed in a mix of 1.8% methylcellulose and 2.3 M sucrose (1:1) according to Liou et al. (1996) and transferred to formvar carbon-coated copper grids. Double immunolabeling was performed as described previously (Slot et al., 1991) with optimal combination of gold particle sizes and sequence of antibodies. Cryosections were incubated with rabbit polyclonal anti-GFP antibody (Invitrogen, catalog number A11122, batch 939-306, dilution 1:150) followed by protein-A-conjugated gold (Slot and Geuze, 1985). A rabbit anti-mouse-IgG antibody was used as a bridging antibody with monoclonal anti-GM130 antibody (Becton Dickinson, catalog number 610823, batch 4324839). After labeling, the sections were treated with 1% glutaraldehyde, counterstained with uranyl acetate and embedded in methyl cellulose uranylacetate (Slot et al., 1991). Electron micrographs were acquired on a Tecnai Spirit electron microscope (FEI, Eindhoven, The Netherlands) equipped with a 4k CCD camera (EMSIS GmbH, Münster, Germany).

Micropatterns

Glass coverslips were activated with plasma before incubation with PEG-polylysine for 1 h. After mask activation with O_3 during 5 min, coverslips were put on the mask, incubated for 5 min in O_3 and then washed. Before seeding cells, coverslips were incubated in fibronectin solution for 30 min.

Acknowledgements

We thank Vincent Fraisier and François Waharte from the PICT-IBiSA Lhomond imaging facility of Institut Curie and Olivier Leroy from the PICT-IBiSA BDD imaging facility of the Institut Curie. The authors also thank the recombinant antibody platform of the Institut Curie. The authors would like to thank Emilie Colin and Arnaud Echard for discussion about the results. We thank Ana Joaquina Jimenez for commenting on the results and for her help with the micro-patterning.

Competing interests

The authors declare no competing or financial interests.

Author contributions

L.F. carried out most of the experiments, analyzed the data and wrote the manuscript. S.D. performed some experiments and electron microscopy experiments. M.R. established the gene-edited GFP–giantin cell line. G.B. and F.P. designed the study, directed the work, analyzed the data and wrote the manuscript.

Funding

Electron microscopy work was supported by the Agence Nationale de la Recherche through the 'Investments for the Future' program (France-BioImaging) [grant number ANR-10-INSB-04]. We acknowledge the BioImaging Cell and Tissue Core Facility of the Institut Curie (PICT-IBiSA), a member of the France-BioImaging national research infrastructure, supported by the CelTisPhyBio Labex [grant number ANR-10-LBX-0038] part of the IDEX PSL [grant number ANR-10-IDEX-0001-02 PSL]. The work in the laboratory of F.P. was supported by the Institut Curie, the Centre National de la Recherche Scientifique (CNRS) and by grants from the Fondation pour la Recherche Médicale [grant numbers DEQ20120323723 and FDT20150532154] and from the Agence Nationale de la Recherche [grant number ANR-12-BSV2-0003-01].

Supplementary information

Supplementary information available online at
http://jcs.biologists.org/lookup/doi/10.1242/jcs.188870.supplemental

References

Boncompain, G., Divoux, S., Gareil, N., de Forges, H., Lescure, A., Latreche, L., Mercanti, V., Jollivet, F., Raposo, G. and Perez, F. (2012). Synchronization of secretory protein traffic in populations of cells. *Nat. Methods* **9**, 493-498.

Chabin-Brion, K., Marceiller, J., Perez, F., Settegrana, C., Drechou, A., Durand, G. and Pous, C. (2001). The Golgi complex is a microtubule-organizing organelle. *Mol. Biol. Cell* **12**, 2047-2060.

Cole, N. B., Sciaky, N., Marotta, A., Song, J. and Lippincott-Schwartz, J. (1996). Golgi dispersal during microtubule disruption: regeneration of Golgi stacks at peripheral endoplasmic reticulum exit sites. *Mol. Biol. Cell* **7**, 631-650.

Conde, C. and Cáceres, A. (2009). Microtubule assembly, organization and dynamics in axons and dendrites. *Nat. Rev. Neurosci.* **10**, 319-332.

Corthesy-Theulaz, I., Pauloin, A. and Pfeffer, S. R. (1992). Cytoplasmic dynein participates in the centrosomal localization of the Golgi complex. *J. Cell Biol.* **118**, 1333-1345.

de Forges, H., Bouissou, A. and Perez, F. (2012). Interplay between microtubule dynamics and intracellular organization. *Int. J. Biochem. Cell Biol.* **44**, 266-274.

Dimitrov, A., Paupe, V., Gueudry, C., Sibarita, J.-B., Raposo, G., Vielemeyer, O., Gilbert, T., Csaba, Z., Attie-Bitach, T., Cormier-Daire, V. et al. (2009). The gene responsible for Dyggve-Melchior-Clausen syndrome encodes a novel peripheral membrane protein dynamically associated with the Golgi apparatus. *Hum. Mol. Genet.* **18**, 440-453.

Efimov, A., Kharitonov, A., Efimova, N., Loncarek, J., Miller, P. M., Andreyeva, N., Gleeson, P., Galjart, N., Maia, A. R. R., McLeod, I. X. et al. (2007). Asymmetric CLASP-dependent nucleation of noncentrosomal microtubules at the trans-Golgi network. *Dev. Cell* **12**, 917-930.

Farquhar, M. G. and Palade, G. E. (1981). The Golgi apparatus (complex)-(1954-1981)-from artifact to center stage. *J. Cell Biol.* **91**, 77s-103s.

Ferraro, F., Kriston-Vizi, J., Metcalf, D. J., Martin-Martin, B., Freeman, J., Burden, J. J., Westmoreland, D., Dyer, C. E., Knight, A. E., Ketteler, R. et al. (2014). A two-tier Golgi-based control of organelle size underpins the functional plasticity of endothelial cells. *Dev. Cell* **29**, 292-304.

Glick, B. S. and Luini, A. (2011). Models for Golgi traffic: a critical assessment. *Cold Spring Harb. Perspect. Biol.* **3**, a005215.

Hirschberg, K., Miller, C. M., Ellenberg, J., Presley, J. F., Siggia, E. D., Phair, R. D. and Lippincott-Schwartz, J. (1998). Kinetic analysis of secretory protein traffic and characterization of golgi to plasma membrane transport intermediates in living cells. *J. Cell Biol.* **143**, 1485-1503.

Ho, W. C., Allan, V. J., van Meer, G., Berger, E. G. and Kreis, T. E. (1989). Reclustering of scattered Golgi elements occurs along microtubules. *Eur. J. Cell Biol.* **48**, 250-263.

Jiang, S., Rhee, S. W., Gleeson, P. A. and Storrie, B. (2006). Capacity of the Golgi apparatus for cargo transport prior to complete assembly. *Mol. Biol. Cell* **17**, 4105-4117.

Jordan, M., Schallhorn, A. and Wurm, F. M. (1996). Transfecting mammalian cells: optimization of critical parameters affecting calcium-phosphate precipitate formation. *Nucleic Acids Res.* **24**, 596-601.

Lavieu, G., Dunlop, M. H., Lerich, A., Zheng, H., Bottanelli, F. and Rothman, J. E. (2014). The Golgi ribbon structure facilitates anterograde transport of large cargoes. *Mol. Biol. Cell* **25**, 3028-3036.

Liou, W., Geuze, H. J. and Slot, J. W. (1996). Improving structural integrity of cryosections for immunogold labeling. *Histochem. Cell Biol.* **106**, 41-58.

Lucocq, J. M. and Warren, G. (1987). Fragmentation and partitioning of the Golgi apparatus during mitosis in HeLa cells. *EMBO J.* **6**, 3239-3246.

Nizak, C., Martin-Lluesma, S., Moutel, S., Roux, A., Kreis, T. E., Goud, B. and Perez, F. (2003). Recombinant antibodies against subcellular fractions used to track endogenous Golgi protein dynamics in vivo. *Traffic* **4**, 739-753.

Nizak, C., Sougrat, R., Jollivet, F., Rambourg, A., Goud, B. and Perez, F. (2004). Golgi inheritance under a block of anterograde and retrograde traffic. *Traffic* **5**, 284-299.

Parczyk, K., Haase, W. and Kondor-Koch, C. (1989). Microtubules are involved in the secretion of proteins at the apical cell surface of the polarized epithelial cell, Madin-Darby canine kidney. *J. Biol. Chem.* **264**, 16837-16846.

Pfeffer, S. R. (2010). How the Golgi works: a cisternal progenitor model. *Proc. Natl. Acad. Sci. USA* **107**, 19614-19618.

Presley, J. F., Cole, N. B., Schroer, T. A., Hirschberg, K., Zaal, K. J. and Lippincott-Schwartz, J. (1997). ER-to-Golgi transport visualized in living cells. *Nature* **389**, 81-85.

Puri, S. and Linstedt, A. D. (2003). Capacity of the golgi apparatus for biogenesis from the endoplasmic reticulum. *Mol. Biol. Cell* **14**, 5011-5018.

Quintyne, N. J., Gill, S. R., Eckley, D. M., Crego, C. L., Compton, D. A. and Schroer, T. A. (1999). Dynactin is required for microtubule anchoring at centrosomes. *J. Cell Biol.* **147**, 321-334.

Rindler, M. J., Ivanov, I. E. and Sabatini, D. D. (1987). Microtubule-acting drugs lead to the nonpolarized delivery of the influenza hemagglutinin to the cell surface of polarized Madin-Darby canine kidney cells. *J. Cell Biol.* **104**, 231-241.

Rivero, S., Cardenas, J., Bornens, M. and Rios, R. M. (2009). Microtubule nucleation at the cis-side of the Golgi apparatus requires AKAP450 and GM130. *EMBO J.* **28**, 1016-1028.

Rogalski, A. A., Bergmann, J. E. and Singer, S. J. (1984). Effect of microtubule assembly status on the intracellular processing and surface expression of an integral protein of the plasma membrane. *J. Cell Biol.* **99**, 1101-1109.

Sandoval, I. V., Bonifacino, J. S., Klausner, R. D., Henkart, M. and Wehland, J. (1984). Role of microtubules in the organization and localization of the Golgi apparatus. *J. Cell Biol.* **99**, 113s-118s.

Schmidt, E. K., Clavarino, G., Ceppi, M. and Pierre, P. (2009). SUnSET, a nonradioactive method to monitor protein synthesis. *Nat. Methods* **6**, 275-277.

Schmoranzer, J., Kreitzer, G. and Simon, S. M. (2003). Migrating fibroblasts perform polarized, microtubule-dependent exocytosis towards the leading edge. *J. Cell Sci.* **116**, 4513-4519.

Sengupta, P., Satpute-Krishnan, P., Seo, A. Y., Burnette, D. T., Patterson, G. H. and Lippincott-Schwartz, J. (2015). ER trapping reveals Golgi enzymes continually revisit the ER through a recycling pathway that controls Golgi organization. *Proc. Natl. Acad. Sci. USA* **112**, E6752-E6761.

Shima, D. T., Cabrera-Poch, N., Pepperkok, R. and Warren, G. (1998). An ordered inheritance strategy for the Golgi apparatus: visualization of mitotic disassembly reveals a role for the mitotic spindle. *J. Cell Biol.* **141**, 955-966.

Slot, J. W. and Geuze, H. J. (1985). A new method of preparing gold probes for multiple-labeling cytochemistry. *Eur. J. Cell Biol.* **38**, 87-93.

Slot, J. W., Geuze, H. J., Gigengack, S., Lienhard, G. E. and James, D. E. (1991). Immuno-localization of the insulin regulatable glucose transporter in brown adipose tissue of the rat. *J. Cell Biol.* **113**, 123-135.

Storrie, B., White, J., Röttger, S., Stelzer, E. H. K., Suganuma, T. and Nilsson, T. (1998). Recycling of golgi-resident glycosyltransferases through the ER reveals a novel pathway and provides an explanation for nocodazole-induced Golgi scattering. *J. Cell Biol.* **143**, 1505-1521.

Sugioka, K. and Sawa, H. (2012). Formation and functions of asymmetric microtubule organization in polarized cells. *Curr. Opin. Cell Biol.* **24**, 517-525.

Van De Moortele, S., Picart, R., Tixier-Vidal, A. and Tougard, C. (1993). Nocodazole and taxol affect subcellular compartments but not secretory activity of GH3B6 prolactin cells. *Eur. J. Cell Biol.* **60**, 217-227.

Watson, P., Forster, R., Palmer, K. J., Pepperkok, R. and Stephens, D. J. (2005). Coupling of ER exit to microtubules through direct interaction of COPII with dynactin. *Nat. Cell Biol.* **7**, 48-55.

Yadav, S., Puri, S. and Linstedt, A. D. (2009). A primary role for Golgi positioning in directed secretion, cell polarity, and wound healing. *Mol. Biol. Cell* **20**, 1728-1736.

Yang, W. and Storrie, B. (1998). Scattered Golgi elements during microtubule disruption are initially enriched in trans-Golgi proteins. *Mol. Biol. Cell* **9**, 191-207.